



# A highly radiative combustion chamber for heavy fuel oil combustion

Rafael Villasenor\*†, Rogelio Escalera

*Instituto de Investigaciones Eléctricas, Departamento de Sistemas de Combustion, 62001 Cuernavaca, Morelos, Mexico*

Received 14 April 1997; in final form 27 December 1997

## Abstract

An experimental study of the effects of secondary air jets injected perpendicular to the flame axis on the combustion of heavy fuel oil was investigated in a cylindrical refractory lined furnace of 500 kW. The design used here directed the secondary air jets at the end of the first stage combustion, thus maximizing the air jet energy and avoiding the unnecessary mixing of air with burned gases in the furnace adopted in low  $\text{NO}_x$  burners. The performance of the new burner design was evaluated by quantifying the exhaust concentration levels of  $\text{CO}$ , and  $\text{NO}_x$ . The experimental results demonstrated that  $\text{NO}_x$  was reduced as much as 70% and practically 100% removal efficiency for  $\text{CO}$ . © 1998 Elsevier Science Ltd. All rights reserved.

## 1. Introduction

Heavy fuel oils of various qualities are used worldwide for power generation. About sixty-five percent of the electricity that is produced in Mexico comes from oil combustion. The composition of the Mexican Heavy Fuel Oil (HFO) differs considerably from those fuels that are burned in the great majority of oil-consumer countries. According to Ruiz [1], a typical Mexican HFO contains asphaltene in relatively high concentrations. An elemental composition analysis of their international counterparts made by Sefer and Moulton [2], on the other hand, indicates a much lower content. In view of that, Mexican heavy fuel oils are among the worst type of fuels for power generation since they are high in asphaltene whose aromatic molecular structure leads to the formation of graphitic combustion residues that are particularly difficult to burn out. This problem is accentuated by the typical low  $\text{NO}_x$  burner configurations using staged combustion with a rich primary zone, since the low  $\text{NO}_x$  must be balanced against increasing  $\text{CO}$  and unburned carbonaceous material.

To date, low-cost techniques, namely staged combustion, as stated by Thompson et al. [3], and Wood [4], are seen as the best available option of all technologies worldwide for reducing  $\text{NO}_x$  production in oil- and coal-firing burners. Postflame reduction techniques are outside the scope of the present investigation. Nonetheless a comment on these techniques comes in order. Post-combustion  $\text{NO}_x$  control refers to flue gas treatment methods that convert or remove  $\text{NO}_x$  species downstream of the furnace. The most common process involves injecting ammonia or urea into the flue gas to reduce  $\text{NO}_x$  to nitrogen or water vapor. The method is called Selective Catalytic Reduction (SCR) if a catalyst is used, and in the absence of one, Selective Noncatalytic Reduction (SNCR). The former is extremely expensive due to the high cost of the catalyst, whereas the latter does not only have temperature limitations but also ammonia in the presence of sulfur-containing flue gases may combine with  $\text{SO}_3$  to form  $\text{NH}_4\text{HSO}_4$ , which can lead to fouling problems. Despite great efforts on research, an optimum device for in-flame techniques have not been developed yet, particularly for HFO burners. Efficient staged combustion requires accurately matching between the fluid dynamics of the burner and the fuel spray. This study is concerned with a new burner design concept that extends the low  $\text{NO}_x$  staged combustion principle by applying the mixing power of the secondary air in the proper place. This burner system thus overcomes the familiar trade-off

\* Present address. Laboratory for Atmospheric Research, Washington State University, Pullman, WA 99163, U.S.A.

† Corresponding author.

between  $\text{NO}_x$  production and completeness of combustion.

The heat transfer mechanism in oil flames has been identified as a condition that affects the rates of nitric oxide production. However, the main formation is governed by maximum flame temperature, quantity of oxidant and residence time [5]. These considerations may suggest that the rates of heating or cooling combustion products in the flame may directly contribute to the final emission of  $\text{NO}_x$ . According to Roslyakov and Zinkina [6] and the available experience [7, 8] gained in coal combustion, the residence time in the temperature zone in which the formation of  $\text{NO}_x$  is possible seems to be the principal factor. It is then plausible to alter the production of  $\text{NO}_x$  through modifications to the aerodynamic flow patterns via heat transfer conditions and manipulations of the internal recirculation zone in the flame.

The lateral injection of secondary air has been identified as the most appropriate method for reducing the  $\text{NO}_x$  production in heavy fuel oil burners. The technique of injecting high-velocity jets into cylindrical combustors is not new. An excellent contribution on the subject was originally provided by the numerical modeling of a three-dimensional combustor by Serag-Eldin and Spalding [9] using a one-step global reaction. Later on in an effort to explain the localized critical zones of the flow structure inside cylindrical coal combustors subjected to co-flow jets with large velocity difference, Zhou et al. [10] developed a multidimensional code. Zhou and co-workers found that a powerful recirculation zone can be induced by the addition of two co-flowing jets into the furnace. The recirculation zone tends to prolong the residence time of the particles avoiding the potential loss of burnout performance. In this line of work Abbas et al. [8] evaluated the influence of near burner region (NBR) aerodynamics on the formation and emission of nitrogen oxides. They found that a significant decrease in the  $\text{NO}$  concentration in the NBR and a substantial decrease in the furnace exit values is observed when the central tube from a single annular orifice (SAO) burner is replaced with a single central orifice (SCO) burner jet of the same cross-sectional area. The study was concentrated on the relative performance of the two burners. A conclusive statement is that the superiority of the SCO burner was entirely due to the longer particles' residence time in a reducing atmosphere, this being the principle of all low  $\text{NO}_x$  burners. In a more recent work Liu et al. [11] investigated the effects of a single high-velocity jet on the combustion of pulverized coal in a small-scale furnace. The jet was found to have significant effects on flame stabilization and a 30% reduction of  $\text{NO}_x$  emissions was attained. In Liu's work the injector was introduced to the combustor chamber through the jet port on the burner quarl where the recirculation zone is confined. The disruption of the aerodynamic flow pattern in the NBR due

to the single jet may have adverse effects on the overall combustion performance, thus curtailing, to some extent, the advantages of adding a secondary air jet at an angle with the axis of symmetry.

The above findings strongly suggest that the NBR aerodynamics of existing combustion facilities can be manipulated to achieve low  $\text{NO}_x$  emission values. Therefore one of the main objectives of this study was to establish the correct point of injection of the air jets into the furnace, in order to achieve the lowest possible levels of  $\text{NO}_x$  and solid particulates while maintaining a high thermal efficiency and burnout performance. The optimum point of injection was determined by directing the secondary air jets progressively at different axial locations of the furnace. Then the corresponding  $\text{NO}_x$  concentration was measured in the flue gases for that particular injection port. The selection of this control technology has been made based on the low cost effectiveness for modifying an existing large-scale furnace in the combustion facility at the Instituto de Investigaciones Electricas (IIE), in Mexico. The conventional swirl burner originally fitted in the 500 kW research furnace at the IIE produced both high  $\text{NO}_x$  and poor burnout of the residual heavy fuel oil. Adapting an International Flame Research Foundation (IFRF) type block swirler [12], rectified the poor dynamics and provided a suitable well mixed shear layer to which the fuel injection could be matched.

In this investigation the material is organized in four sections including the introduction. The second section explains the configuration of the combustion chamber and its various components. The instruments that measure mean velocity are described in section three. The experimental results for the new burner configuration are discussed also in the third section along with the equipment used for measuring the heat flux,  $\text{NO}_x$ ,  $\text{CO}$ , and solid residues. Finally, the last section contains relevant conclusions and future work.

## 2. Experimental furnace

The combustion tests were performed on a horizontally oriented furnace, located in the combustion facility at the Instituto de Investigaciones Electricas (IIE), in Mexico. The complete design and manufacturing of the combustion chamber has been done at IIE resulting in a cylindrical furnace of internal diameter 0.89 m, and 3.0 m long, as Fig. 1 shows. The furnace is large enough to ensure fully turbulent flow combined with significant thermal radiation transfer, but small enough to enable trials to be performed at an acceptable cost. The furnace's inner layer is 0.115 m thick built with refractory brick that can withstand temperatures of up to 1600°C. The inner wall of the burner is separated by an outer enclosing air jacket and a blanket of ceramic fiber 0.025 m thick.

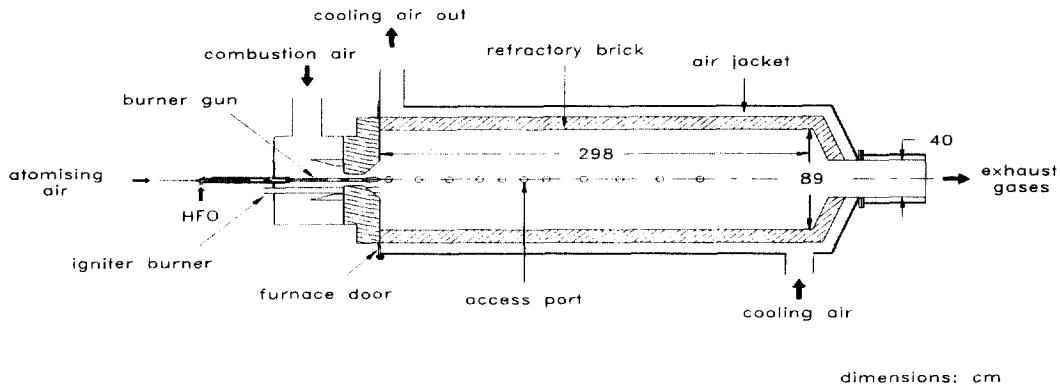


Fig. 1. Schematic of the furnace.

The sets of measurements taken at the experimental site were collected after extensive modification to the furnace layout. Before the present investigation was undertaken the original combustion chamber burned HFO with the purpose of studying the chemistry of flue gas analogous to that produced in a utility boiler. A major modification to the furnace was the implementation of a swirler disk attached at the burner throat. The dimensions of the swirler were carefully chosen to properly shorten or enlarge the recirculation zone by creating a toroidal vortex, thus improving the symmetry in the flow, and providing a continuous source of heat to evaporate the fuel droplets followed by ignition. The advantage of using such a swirler plate stems from its simple installation, since the combustion system does not require significant modification. To further improve the symmetry of the injected air flow for combustion into the swirler pre-chamber, an alteration in the tangential duct entrance was also performed. The swirl generator that has been designed is a movable-block type. The specifications for constructing this kind of swirlers are reported in the literature by Beér and Chigier [12].

In experiments such as the one described here it is necessary to have an adequate flame symmetry and repeatability. Although the presence of a tangential component of the velocity vector is not sufficient to ensure repeatability of the data, axisymmetric flow conditions are guaranteed as was corroborated by the mean axial and tangential velocity measurements taken after the installation of the swirler disk. While it is recognized that the flow field during combustion will be different than during these cold flow tests, the tests were designed to measure the effects of the above modifications on a relative, semiquantitative basis for trend evaluation. The velocity measurements are discussed in a later section.

One significant difference of IIE's combustion chamber relative to other furnaces, particularly the Imperial College furnace described by Hassan et al. [13], is the form in which the walls are cooled. Conventional experimental

furnaces use water-cooled steel segments whereas an air jacket surrounding the refractory brick of IIE's furnace has been adapted for cooling purposes. In general a HFO flame in a highly radiative furnace exhibits the same basic structure as those flames confined in furnaces that use more effective ways of removing heat from their walls. However the flame-to-wall interaction becomes obvious by looking at the temperature profiles that carry the footprint of the various chemical processes that take place within the flame.

The heavy fuel oil burner gun used throughout the investigation operated with a removable internal twin fluid atomizer. The single orifice atomizer houses an internal mixing chamber. In these kind of atomizers the air and fuel are piped separately to the nozzle and mixed just before they enter the atomizing slots. To produce a uniform discharge through the orifice the pressurized air is mixed thoroughly with the fuel in a swirl chamber before the fluids are ejected from the atomizer. A full spray characterization was done as an independent study. The performance of the atomizer was quantified over a wide range of oil and air flow rates. The spray characteristics that were measured included the Sauter Mean Diameter (SMD) at seven radial positions, the spray angle and the spray radial distribution.

The burner is mounted in such a way that the flame develops along the chamber axis. The burner has a quarl expansion of 1.3 (throat diameter of 0.11 m and outer diameter of 0.143 m) and was made out of refractory cement. The downstream end of the chamber is connected to a train of five air-cooled heat exchangers each of 0.4 m internal diameter and 5 m in total length. Once the temperature of the flue gas has been reduced, the combustion mixture is emitted to the atmosphere through a chimney of 20 m height. The purpose of this train device is to simulate the flue-gas temperature profile of a full-scale utility boiler.

A complete description of the flow variables in a combustion chamber is essential to any study of combustion

pollutant formation. This is a monumental task that can be performed once the correct operating conditions that are required for maximizing the furnace thermal efficiency have been established. A partial characterization of the furnace has been accomplished by evaluating the aerodynamics of cold flow tests and measuring the flame temperature of HFO combustion. The axial and tangential velocity components as well as the flame temperature can be used as indicators to define the turbulent flame structure inside the highly radiative combustion chamber. In doing so, the new burner design is optimized by minimizing the  $\text{NO}_x$  and particulate matter in the stack. The locus of  $\text{NO}_x$  and solid residue is found by varying the position of secondary air jets injected perpendicular to the flame center line. The experimental procedure adopted here to carry out the above tasks is discussed next.

### 3. Results

#### 3.1. Axial and tangential velocity components

To ensure symmetry of the flow in the horizontal furnace the axial and tangential velocity components have been measured radially at several axial stations. The series of cold flow tests are performed by replacing the fuel with atmospheric air. The combustion air flow rate is measured with a previously calibrated orifice plate. The mass flow rate is kept in the range from 600–608 kg/h. Static pressure measurements are made with the aid of a disk probe. A Hubbard probe is used to detect the location of the reverse flow zones while a five-hole Pitot tube is positioned according to the direction of flow previously registered. The calibration of the probe was performed inside a wind tunnel. In the wind tunnel the probe was allowed to rotate by varying the azimuthal angle around the vertical axis of the horizontal support. The standard calibration method is well documented in the literature and the estimated uncertainties in this case were not larger than 5%.

Two quarl-half angles have been tested for trend evaluation ( $25^\circ$  and  $30^\circ$ ). The angles were chosen based on the internal furnace diameter and the type of atomizer used during the trials. In Figs 2 and 3 the velocity profiles for a representative swirl number of 0.7 are shown at three axial locations. The static pressure profile (not shown) and the velocity profiles were radially measured every three centimeters from the burner's center line to the wall. The experimental data were taken through the side ports of the furnace. Each port for viewing and probing has an internal diameter of 0.056 m.

The reverse flow region in Figs 2 and 3 appears as the dotted line that forms the closed loop. The bounded region encloses the toroidal vortex ring that defines the internal recirculation of hot combusted products. A wider

recirculation zone is produced when the burner is aligned through the  $30^\circ$  quarl-half angle. This behavior is anticipated since the flow exiting the burner throat encounters less obstruction. The radial profiles of the axial velocity component at locations greater than 47.5 cm were found to be oriented in the main direction of flow, indicating the presence of a fully developed region. Since the purpose of measuring the flow velocity was to ensure symmetry conditions and to establish the approximate dimensions of the recirculation zone in the central parts of the flow, no experimental data on velocity are reported after the fully developed flow region is reached. For swirl numbers up to 0.9 the vortex ring never crosses the plane at 69 cm from the burner's wall.

It is important to observe that the axial velocity profiles in Figs 2 and 3 are symmetrical regarding the burner central line, whereas the tangential velocity presents a typical inflection point situated on the edge of the toroidal vortex ring. The characterization of the flame structure has been effected by using the  $25^\circ$  quarl-half angle. The decision has been made on the matching angles between the spray produced by the atomizer and the combustion air passing through the burner's throat. Thus under these conditions the air flow is expected to enhance the mixing rates and produce a more uniform vaporization of fuel droplets.

#### 3.2. $\text{NO}_x$ and particulate matter

One of the key factors for increasing combustion efficiency is dependent on the fuel-air mixing. A deficient internal recirculation zone, which supplies the energy for ignition, can lead to large quantities of pollutants. The strength and size of the mixing region can be varied by adjusting the tangential component of the velocity vector. The magnitude of the tangential component of the velocity vector is controlled by regulating the degree of swirl imparted to the flow. By keeping the atomizing air to fuel ratio fixed and maintaining the other relevant operational parameters, like quarl's half-angle constant, it is possible to construct a curve that indicates the amount of  $\text{NO}_x$  in the flue gas as a function of swirl. Figure 4 presents a comparison between previous experimental data reported by Barreiros et al. [14] with the measurements taken at IIE. Figure 4 shows that both distributions decay as the swirl number increases. However, the  $\text{NO}_x$  measured in the present study reaches even lower levels for swirl numbers of practical importance in this investigation ranging from 0.6–0.9. Increasing the swirl number above 0.9 yields smaller amounts of  $\text{NO}_x$  to be formed for the flame conditions reported by the other authors. Although no measurements were taken for swirl numbers well above 1.0, it is clear from Fig. 4 that the IIE furnace tends to produce more  $\text{NO}_x$  as the degree of swirl rises. This behavior is consistent, however, with the highly radiative

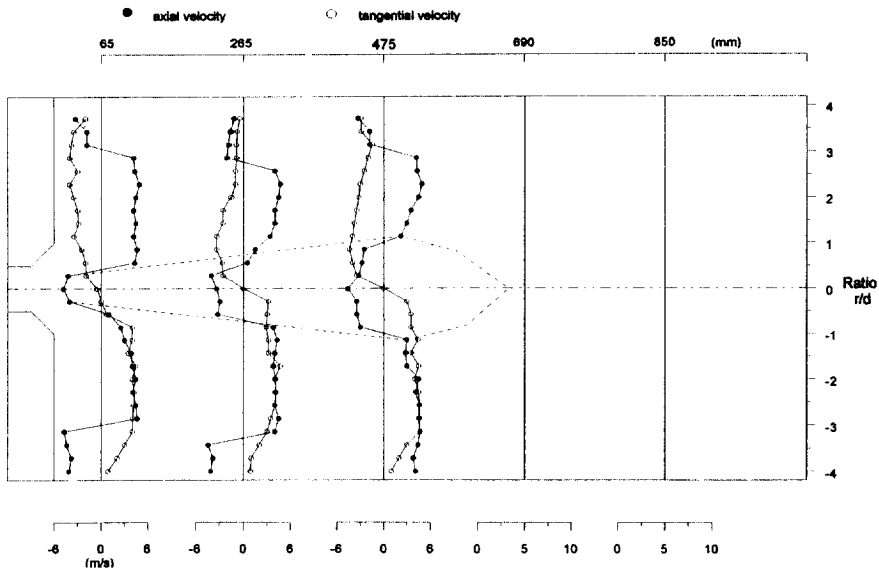


Fig. 2. Axial and tangential velocity profiles for a swirl number of 0.7 and a quarter-half angle of 25°.

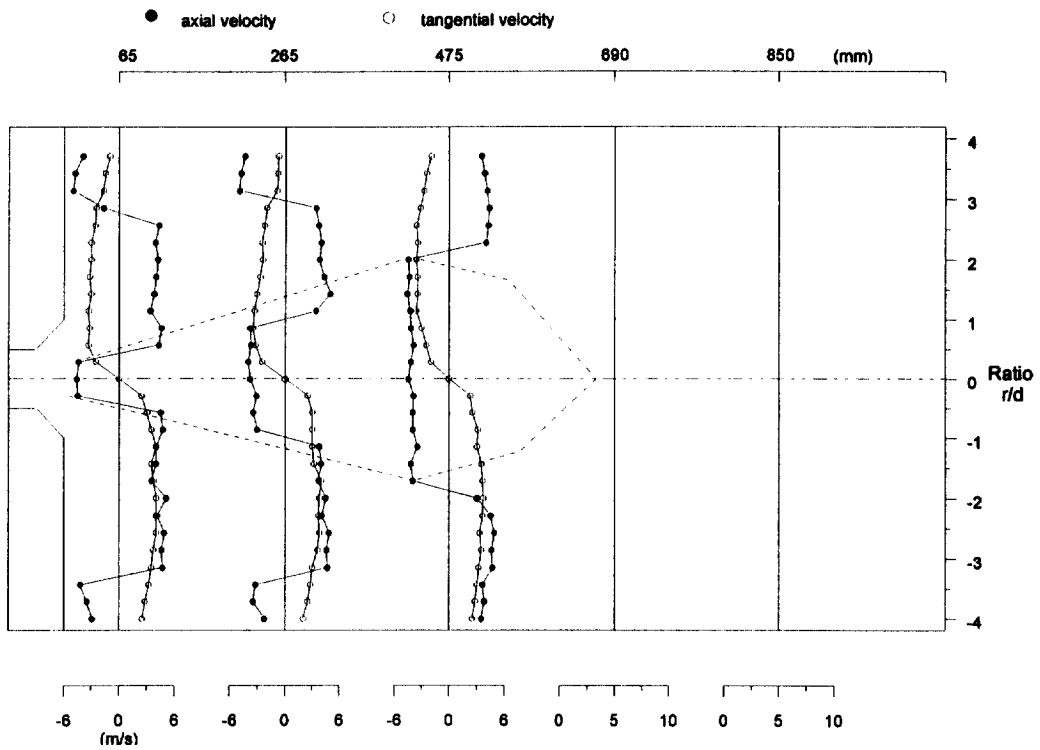


Fig. 3. Axial and tangential velocity profiles for a swirl number of 0.7 and a quarter-half angle of 30°.

properties of the IIE combustion chamber due to its poor heat transfer removal capacity.

The incident wall radiation flux, which plays a definite role in the formation and destruction of  $\text{NO}_x$  and minor

species as well, was also measured as a function of axial distance for different swirl numbers, including the case without the swirler plate. The measurements were taken after the furnace operational parameters became inde-

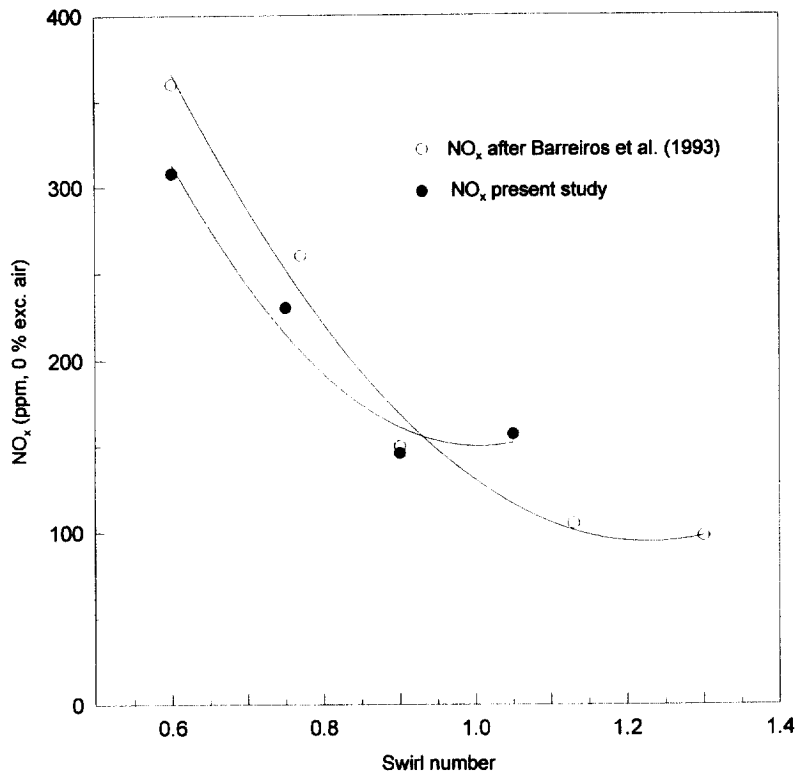


Fig. 4. Influence of swirl number on measured NO<sub>x</sub> emissions.

pendent of time. The furnace burned 36 kg/h of HFO with 0.5% of excess O<sub>2</sub> content and a 0.1 air to fuel mass ratio. The fuel flow rate suitable for this and other trials were determined from the flow characteristic curves of the internal twin fluid atomizer. The wall radiation flux was sampled over a number of intervals sweeping the full length of the combustion chamber. The probe used was a LAND portable heat flux meter developed by Central Electricity Research Laboratories (CERL). The accuracy of the fluxprobe is 5% of the measured value.

Four swirl numbers were considered (0.1, 0.4, 0.75 and 1.0) in addition to the spray combustion test that has poor flame stabilization characteristics due to the absence of a swirler plate. Figure 5 shows the incident wall radiation sampled at eleven axial positions. The solid lines in Fig. 5 are continuous functions obtained from the data points with a smoothing fit. It is important to identify that all five distributions present a maximum whose position is highly dependent on the tangential component of velocity. However, the greatest incident radiation on the furnace's wall was measured for the flame with a zero tangential velocity, this being the most radiant flame. The location and size of the crest are an indication of the position and strength of the reaction zone. Without the swirler plate the reaction zone extends from the burner

to about eight burner throat diameters downstream. Thereafter combustion ceases and the corresponding decrease in incident wall radiation is obtained. When swirl is imparted to the flow the relative position of the peak is changed without following a pattern consistent with the magnitude of the swirl number. Although such behavior does not obey a simple recurrence relation some basic features about the given tendency may be deduced from Fig. 5. For the 0.1 swirl number flame the incident wall radiation attains a smooth peak at approximately  $x/d = 7$ . According to visual observations this flame turned out to be the longest and more distant from the burner exit. Increasing the swirl number without exceeding 0.75 causes the crest to move closer to the burner leading to even larger radiation levels. One can infer from such a trend that droplet evaporation takes place at a faster rate by going from a 0.1 to a 0.75 swirl number flame, thus improving combustion efficiency. Augmenting the swirl number beyond 0.75 shifts the crest farther away from the burner with a subsequent reduction in the radiant potency of the flame. This is explained by noticing that the length of the toroidal vortex ring tends to be enlarged as the swirl number increases. As the mixing recirculation zone amplifies the oil droplets spend prolonged times in the primary reaction zone before they

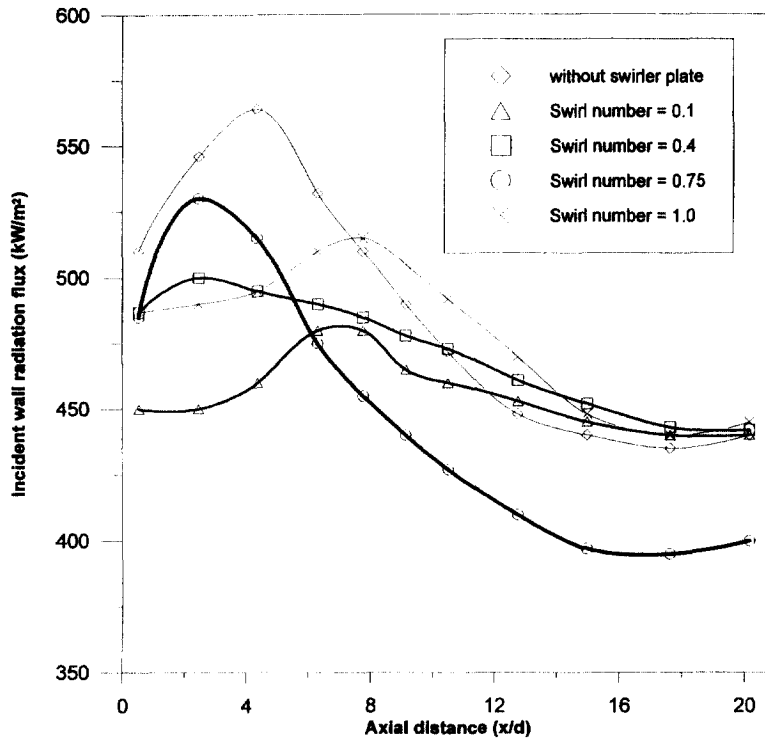


Fig. 5. Incident wall radiation flux for 36 kg/h of HFO flow rate and 0.5% of excess  $O_2$  content.

start to burn. When they have completely evaporated combustion takes over with the corresponding heat release that coincides with the radiation peak. Notice also that the incident radiation decays abruptly for a swirl number of 0.75, but converges to approximately 450  $kW/m^2$  for the other four cases.

It is important to point out that an equivalent combustion test was carried out on the combustion chamber at the Imperial College by Costa et al. [15] using a similar probe. Both furnaces have about the same length. Their results are similar in the region close to the burner but the incident wall radiation at the far end of their furnace is approximately three times lower than the reported value in this study. This discrepancy confirms that the cooling systems that each furnace uses plays a central role in changing the flame structure in both, the radiative and convective sections of the combustion chamber.

A series of combustion tests was effected to quantify the total  $NO_x$  production measured in the stack, while injecting air jets perpendicularly to the axis of symmetry of the combustion chamber. The basis for discussion rests on the fact that a second highly turbulence intensity zone is produced by the injection of the secondary air jets. One of the main advantages of this flow configuration arrangement is that low values of the flame temperature can be achieved decreasing thermal  $NO_x$  production accordingly. In this experiment the secondary air at room

temperature was directed perpendicular to the flame axis. On each combustion test the secondary air was supplied through a single pair of probing ports placed on the lateral surface of the furnace. There were eleven probing port pairs distributed evenly along the side of the furnace. The convention adopted here is that the first and last probing ports are located at the two ends of the furnace, being probing port one closest to the burner, as Fig. 6 shows. The effectiveness of the present  $NO_x$  reduction method was measured relative to a combustion test performed as a base line under stable operating conditions without the air jets. The furnace operating conditions and the properties of the heavy fuel oil used during the combustion tests, are shown in Tables 1 and 2, respectively.

Figure 7 shows the measured  $NO_x$  at the stack corresponding to various positions of the injected secondary air jets. The  $NO_x$  base line is also graphically represented in Fig. 7 and is used here as a relative measure for observing the advantages of the new burner design. The measured  $NO_x$  in the base line test yielded 316 ppm. The benefit of reducing the  $NO_x$  formation by supplying part of the air for combustion through lateral ports is seen to be not satisfactory for regions closer to the burner. However, for the fifth and subsequent probing ports there seem to be a remarkable  $NO_x$  reduction. The  $NO_x$  distribution indicates that the effects of the air jets on the

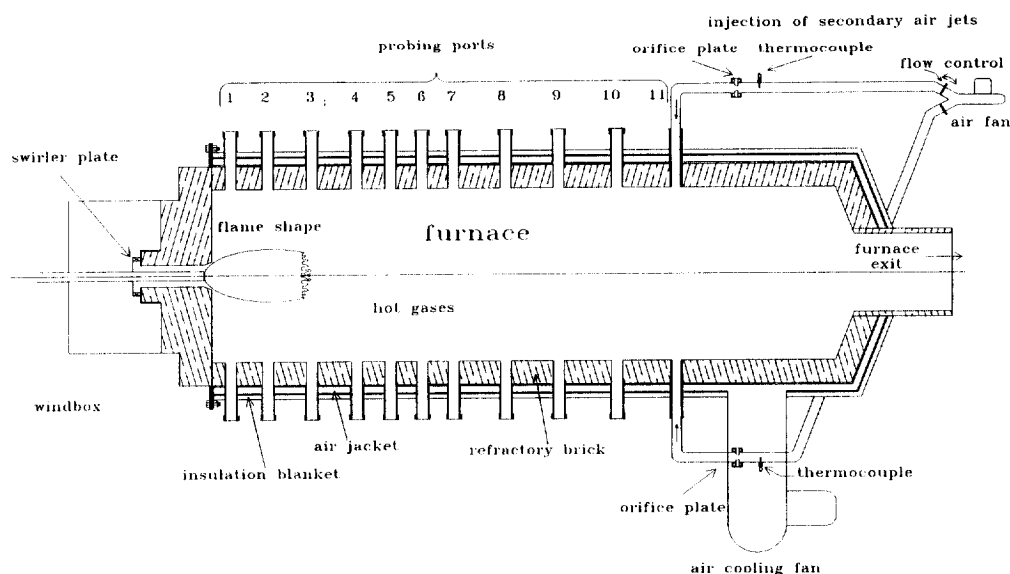


Fig. 6. Schematic diagram of the furnace showing the secondary air injection through the 11 probing port.

Table 1  
Furnace operating conditions

Variables	Without sec. air injection	With sec. air injection
Heavy-fuel-oil flow rate ( $\text{kg h}^{-1}$ )	28	28
Combustion air flow rate ( $\text{kg h}^{-1}$ )	450	274
Secondary air flow rate ( $\text{kg h}^{-1}$ )	—	176
Pressure of the atomizing air* (bar)	1.4	1.4
Temperature of the atomizing air* ( $^{\circ}\text{C}$ )	35.5	35.1
Pressure of the heavy-fuel-oil* (bar)	1.6	1.6
Temperature of the heavy-fuel-oil* ( $^{\circ}\text{C}$ )	120	120
Temperature of the combustion air ( $^{\circ}\text{C}$ )	34	34
Furnace wall temperature† ( $^{\circ}\text{C}$ )	1290	1227
Swirl number meas. at the burner's throat	0.75	0.75
Room temperature ( $^{\circ}\text{C}$ )	31	31

\* Measured at the burner entrance.

† Measured at the probing port no. 9, at a distance of 5 cm. from the wall, inside the furnace.

$\text{NO}_x$  levels are immaterial for port number five and beyond.

The performance of this burner design is also verified by quantifying the disappearance of solid carbonaceous material. Particulate matter was measured at the stack for secondary air injected at three locations. The particulate levels with and without the secondary air jets are also shown in Fig. 7. It is inferred by looking at these two sets of data points that an adverse effect on the particulate concentration prevails even with the use of the injected air jets. Even though the particulate emission tends to be

reduced when the secondary air is supplied through the very far probing ports, the concentration is still high relative to the particulate base line. It may be extrapolated from this trend that the desired concentration level of solid residue could be attained by enlarging the combustion chamber. A longer combustion chamber means higher residence times but also higher costs or even space limitations, both of which are to be avoided. One feasible way of reducing both  $\text{NO}_x$  and particulate matter without increasing the cost too much is to inject the air at a temperature well above the ambient temperature. With



Table 2  
Properties of heavy fuel oil used during the combustion tests

Property	Value
Density at 1 atm and 20°C (kg m <sup>-3</sup> )	982
Surface tension at 20°C (N m <sup>-1</sup> )	0.034
Dynamic viscosity (N s m <sup>-2</sup> ):	
at 50°C	1.0
at 60°C	0.5
at 82.2°C	0.16
Conradson carbon residue (% wt)	15
Asphaltenes (% wt)	15
Elemental analysis (% wt)	
Carbon	84.5
Hydrogen	10.71
Sulfur	3.75
Oxygen	0.15
Nitrogen	0.37
Ash	0.073
Gross calorific value (MJ kg <sup>-1</sup> )	42.57

hotter secondary air jets the particulate emission curve depicted in Fig. 7 will decay suddenly yielding lower concentration levels of solid residues. It is very likely that with a change in the thermal characteristics of the jets

the NO<sub>x</sub> distribution would suffer a slight modification, although not very significant from the one shown in Fig. 7. The optimum zone of operation of the 500 kW furnace can thus be determined.

In this study the emissions of O<sub>2</sub>, CO and NO<sub>x</sub> were measured by means of a LAND analyzer model Lancom 6500 (Sheffield, U.K.), with an accuracy of 1% for O<sub>2</sub> and 4% for CO and NO<sub>x</sub>. In the method of analysis the gas sample was extracted through a 9 mm ID stainless steel tube near the stack inlet. Before reaching the analyzer, the gas sample was conditioned through two stages of drying and filtering. The analyzer had an analogue output signal of 4–20 mA that was connected to a data logger to record the measurements. The data logger was the interface between the analyzer and a notebook computer where the complete test was observed through the real time graph display.

The particulates were measured with a universal stack sampler (Andersen Instruments, U.S.A.) which was designed to sample gas stream effluents isokinetically according to Environmental Protection Agency standards. Stack gases are extracted through a nozzle and a heated probe into a heated filter chamber where the particulates are removed. The hot gases are then passed through a series of cold impingers where condensables are removed and the gases are cooled before going into the pump, the dry gas meter, and the flow sensing orifice.

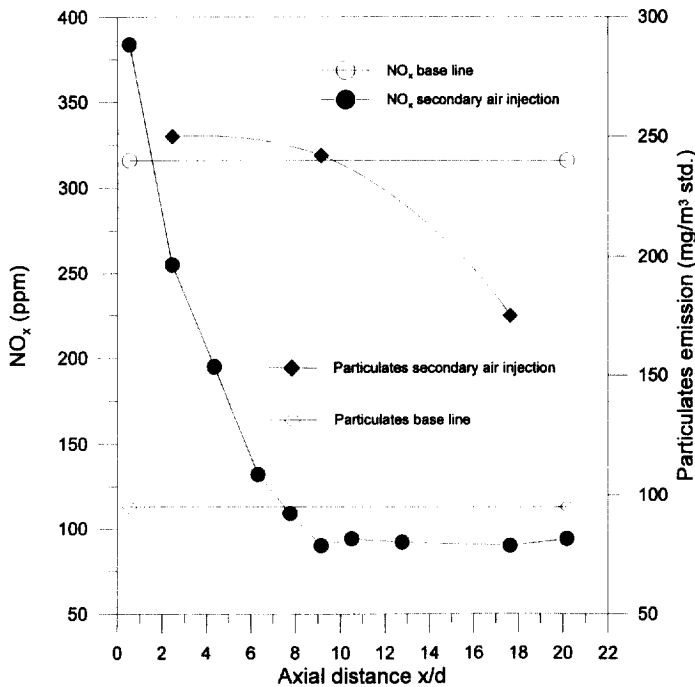


Fig. 7. Comparison of the NO<sub>x</sub> emissions measurements in the stack with and without air injection.

The particulates are determined by method 5 as outlined in the Federal Register Vol. 40, 1994. The estimated accuracy of method 5 is 12%.

3.3. Radial temperature profiles

Detailed measurements of radial flame temperature were measured without feeding the lateral secondary air. The purpose of measuring the flame temperature was to examine the distribution of steep temperature gradients due to the highly radiative properties of the furnace. The experimental temperature data included the near-burner field of the combustion chamber. The temperature profiles were measured by means of a suction pyrometer over a number of intervals sweeping the section of the furnace from  $x/d = 6.32$  to 17.64. The suction pyrometer, inserted through six probing ports, corresponds to an International Flame Research Foundation (IFRF) design.

Figure 8 shows the temperature profiles along six probing ports, corresponding to  $x/d$  of 6.32, 7.77, 9.14, 10.5, 12.77 and 17.64, where  $d = 110$  mm. The six profiles are highly symmetrical to the furnace center line, despite the fact that the furnace is horizontally oriented. The suction pyrometer cannot stay embedded into the flame for longer periods of time. Long exposure causes the burning droplets of HFO to suddenly condense inside the gas suction line, causing severe fouling in the suction passages and outside the cooling probe. This situation explains why the first measured temperature profile occurred at  $x/d = 6.32$ .

It can be seen in Fig. 8 that the flame presents steep

temperature gradients within the toroidal vortex ring. A rapid attenuation of the strength of the combustion processes is detected outside the central recirculation zone of the turbulent spray flame. This is deduced by the fairly flat radial flame temperature distributions in the middle section of the chamber. Farther down from the flame tip the temperature profiles showed only axial variations with a rather uniform temperature distribution at every axial plane. The flame tip of the turbulent flame was observed in the section of the furnace limited by the axial planes located at  $x/d = 7.77$  and  $x/d = 9.14$

4. Conclusions

The effects of secondary air jets were definitely found to play a significant role in the reduction of  $NO_x$  and elimination of practically 100% of the CO produced during combustion. A 71%  $NO_x$  decrease was attained with the new burner configuration. The desired reduction levels of particulate emissions were not satisfactory, in fact, they turned out to be well above the base line values. However, a feasible way to lowering the carbonaceous material can be achieved by changing the thermal input of the secondary air jets, while maintaining optimum combustion efficiencies. The injection of hotter secondary air is believed to significantly decrease the particulate emission levels without severely curtailing the positive effects obtained in the reduction of the  $NO_x$  concentration. The decision of rising the secondary air temperature is extrapolated from the fact that the jets of

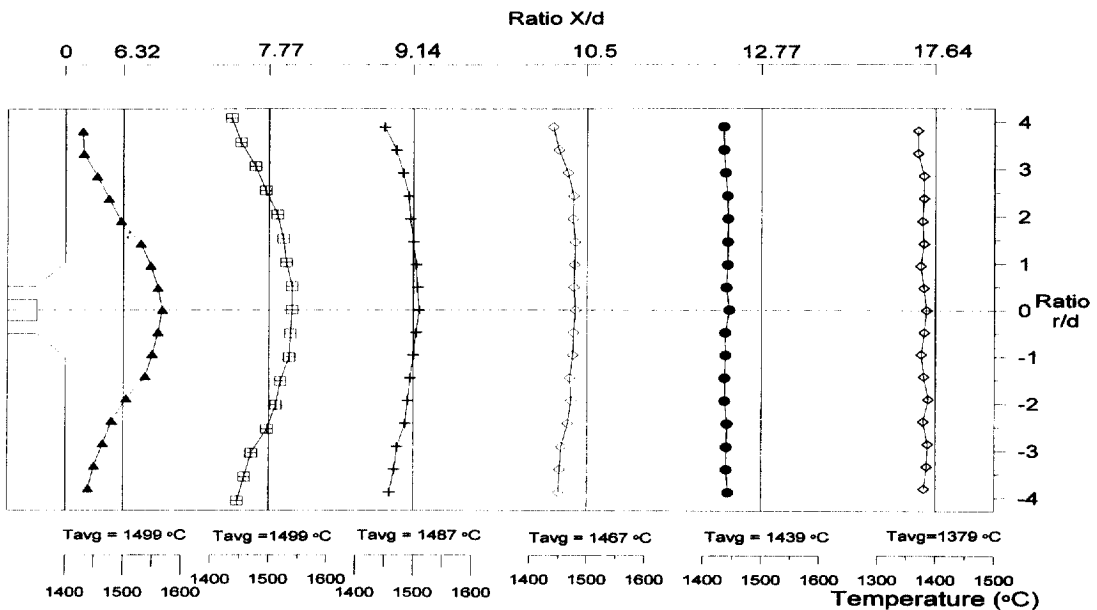


Fig. 8. Temperature profiles for a swirl number of 0.75, HFO flow rate of 28 kg/h and an excess  $O_2$  content of 1.0%.

ambient air produce a decline in the enthalpy of the flue gas after being mixed with the products of combustion. Hence the net destruction of particulate matter tends to be more temperature sensitive. An adequate air jet temperature will oxidize the right amount of particulate matter to reach the optimum operational point. The optimum operational point is defined here as that which results at the intersection between the  $\text{NO}_x$  curve and the particulate emission curve.

Although the features commonly found in other similar burners and those embedded in the IIE burner do not seem to modify considerably the ordinary flow pattern, the flame structure and the combustion processes are definitely affected by the injection of air jets. Therefore the secondary air injection technique is highly promising to the industrial furnace application. It is a low-cost and simple implementation technique that should be considered in future burner designs.

Further improvements to reducing both  $\text{NO}_x$  and particulate matter in a more effective way include the injection of four lateral hot air jets. The addition of two extra jets is thought to result not only in a more uniform distribution of the secondary air but also in stronger turbulent mixing rates. Another alternative for reducing  $\text{NO}_x$  and particulate matter simultaneously is to premix the flue gas with ambient air and feed the gaseous mixture into the furnace. All these issues are now being undertaken as the second step towards a complete characterization of HFO combustion with high asphaltene content. It is also acknowledged here that a full characterization of a turbulent spray flame demands knowledge of in-flame concentration distributions such as  $\text{O}_2$ ,  $\text{CO}$ ,  $\text{NO}_x$ ,  $\text{CO}_2$  and unburned hydrocarbons. This is a more demanding effort that will be considered in the near future.

#### Acknowledgment

The authors are thankful to Prof. Jim Swithenbank of the University of Sheffield for his valuable comments during the progress of this investigation.

#### References

- [1] Ruiz G. Caracterización de Combustibles y Gas Natural Utilizados en Generadores de Vapor. Instituto de Investigaciones Electricas, Cuernavaca, Morelos, Mexico, IIE/12/1675/1 06/FVI, Final Report, 1983, 1-53.
- [2] Sefer NR, Moulton DS. Residual Fuel Oil User's Guidebook, Vol. 1, Residual Oil Fundamentals, EPRI AP-5826, Final Report, 1988.
- [3] Thompson RE, Shiimoto GH, Muzio LJ. Residual Fuel Oil User's Guidebook, Vol. 2, Residual Oil-Fired Boilers, EPRI AP-5826. Final Report, 1988.
- [4] Wood SC. Select the right  $\text{NO}_x$  control technology. Chemical Engineering Progress 1994;90(1):32-38.
- [5] Tager SA, Halmaru AM. Theoretical evaluation of the effect of certain operational factors on the formation of nitrogen oxides when burning oil. Thermal Engineering 1978;25:37-32.
- [6] Roslyakov RV, Zinkina VN. The effect of heat transfer conditions in furnace chambers on formation of thermal nitric oxide. Thermal Engineering 1991;32:690-3.
- [7] Costa M, Costen P, Lockwood FC. Pulverized-coal and heavy-fuel-oil flames: large-scale experimental studies at Imperial College, London. Journal of the Institute of Energy 1991;64:64-76.
- [8] Abbas T, Costen P, Lockwood FC. The influence of near burner region aerodynamics on the formation and emission of nitrogen oxides in a pulverized coal-fired furnace. Combustion and Flame 1991;91:346-63.
- [9] Serag-Eldin, Spalding DB. Computations of three-dimensional gas-turbine combustion chamber flows. Journal of Engineering for Power 1979;101:327-36.
- [10] Zhou L, Lin W, Zhang J, Wang Z. Numerical modeling of three-dimensional flow field and two dimensional coal combustion in a cylindrical combustor of co-flow jets with large velocity difference. 21st Symp. (Int.) on Combustion. The Combustion Institute 1986:257-64.
- [11] Liu F, Garbett ES, Swithenbank J. The effects of a single high-velocity jet on the combustion of pulverized coal in a small-scale furnace. Journal of the Institute of Energy 1992;24-30.
- [12] Beér JM, Chigier NA. Combustion Aerodynamics, Reprint Edn, Florida: Robert E. Krieger Publishing Company, Inc., 1983, 125.
- [13] Hassan MA, Lockwood FC, Moneib HA. Measurements in a gas-fired furnace. Combustion and Flame 1983;51:249.
- [14] Barreiros A, Carvalho MG, Costa M, Lockwood FC. Prediction of the near burner region and measurements of  $\text{NO}_x$  and particulate emissions in heavy fuel oil spray flames. Combustion and Flame 1993;92:231-40.
- [15] Costa M, Costen P, Lockwood FC. Combustion measurements in a heavy-fuel oil fired furnace. Combustion Science and Technology 1991;75:129-54.